Ecological Modelling 257 (2013) 101–112

Contents lists available at SciVerse ScienceDirect

Ecological Modelling

journal homepage: www.elsevier.com/locate/ecolmodel

Modeling the pH in the tidal fresh Potomac River under conditions of varying hydrology and loads

Carl F. Cerco[a,*], Tammy Threadgill[a], Mark R. Noel[a], Scott Hinz[b]

[a] Environmental Laboratory, US Army Engineer Research and Development Center, 3909 Halls Ferry Road, Vicksburg, MS 39180, USA
[b] Limnotech Incorporated, 4008 Greystone Drive, Austin, TX 78731, USA

ARTICLE INFO

Article history:
Received 15 June 2012
Received in revised form 2 January 2013
Accepted 12 February 2013

Keywords:
pH
Alkalinity
Carbonate cycle
Potomac River
Cyanobacteria

ABSTRACT

The pH of the freshwater portion of the Potomac River estuary attains 9–10.5, driven by photosynthesis during cyanobacteria blooms. Processes which contribute to elevated pH are examined by adding a mass-balance model of the carbonate cycle to an existing eutrophication model. Four new variables are added to the model suite: alkalinity, total inorganic carbon, total calcium, and calcium carbonate. The pH is computed from these four quantities via equilibrium kinetics. The model is employed in a continuous simulation of the years 1994–2000. Emphasis in examination of model results is placed on the tidal fresh portion of the system where elevated pH is an environmental concern. Model sensitivity analysis indicates hydrology has the greatest influence on pH. During low-flow periods, residence time is lengthy allowing ample time for algal production to occur. The production stimulates net uptake of TIC, and results in enhanced pH.

Published by Elsevier B.V.

1. Introduction

The pH of surface waters impacts biological activity and is, in turn, influenced by biologically mediated processes (Soetaert et al., 2007; Weber and Stumm, 1963). Anthropogenic influences, combined with biological activity, can cause pH to deviate significantly from the equilibrium value determined by natural levels of CO_2 in the atmosphere and alkalinity in surface waters. Acid rain deposited in watersheds and water bodies can result in significant reduction of pH in poorly buffered waters (Lung, 1987; Nikolaidis et al., 1989). More recent concerns about acidification focus on the effects of long-term increases in atmospheric CO_2 (Caldeira and Wickett, 2003; Omstedt et al., 2009; Borges and Gypens, 2010). Anthropogenic eutrophication can decrease or increase pH, depending on the predominance of oxidation of organic matter or primary production stimulated by nutrient inputs (Brasse et al., 2002; Hunt et al., 2011; Omstedt et al., 2009). Excess primary production, stimulated by nutrient loads, can produce pH high enough to be toxic to aquatic organisms (Passell et al., 2007; references therein).

The waters of the Chesapeake Bay, USA, and its tidal tributaries are subject to multiple stresses associated with pH fluctuations and trends. The pH of polyhaline waters is decreasing (Waldbusser et al., 2011a), enhancing the dissolution rate of oyster shells and deterioration of oyster reefs (Waldbusser et al., 2011b). Within the tidal freshwater portions of tributaries, the pH trend is opposite. The pH of several systems (Bailey et al., 2006; Gao et al., 2012) attains 9–10.5, driven by photosynthesis during cyanobacteria blooms. The tidal fresh Potomac River (TFPR, Fig. 1) is one of the Chesapeake tributaries subject to elevated pH. Nearly 30 years ago, the TFPR experienced an algal bloom of historic proportions (Thomann et al., 1985) which confounded expectations based on preceding reductions in wastewater phosphorus loading. Consensus focused on the role of a positive feedback mechanism in fueling the bloom. Cyanobacteria photosynthesis increased pH, stripping phosphorus from bottom sediments, thereby stimulating additional photosynthesis, higher pH, and additional phosphorus release. The proposed mechanism was subsequently validated through laboratory experiments (Seitzinger, 1991) and mass-balance modeling (Cerco, 1988) and has since been observed elsewhere in the bay system (Gao et al., 2012). Although the magnitude of the historic bloom has not been repeated, the TFPR is subject to recurrent cyanobacteria blooms and elevated pH.

Determination of the primary factors responsible for the blooms and of potential remedies is perplexing due to the myriad influences, their interactions, and opposing effects (Fig. 2). Algal blooms are stimulated by nutrients from the watershed and from point-source wastewater discharges. Watershed nutrient loads covary with runoff, however. During high-load periods, the water column is turbulent and the system residence time is reduced, discouraging the dominance of cyanobacteria over other algae (Krogmann

* Corresponding author. Tel.: +1 601 634 4207; fax: +1 601 634 3129.
E-mail addresses: carl.f.cerco@usace.army.mil (C.F. Cerco), tammy.l.threadgill@usace.army.mil (T. Threadgill), mark.r.noel@usace.army.mil (M.R. Noel), shinz@limno.com (S. Hinz).

0304-3800/$ – see front matter. Published by Elsevier B.V.
http://dx.doi.org/10.1016/j.ecolmodel.2013.02.011

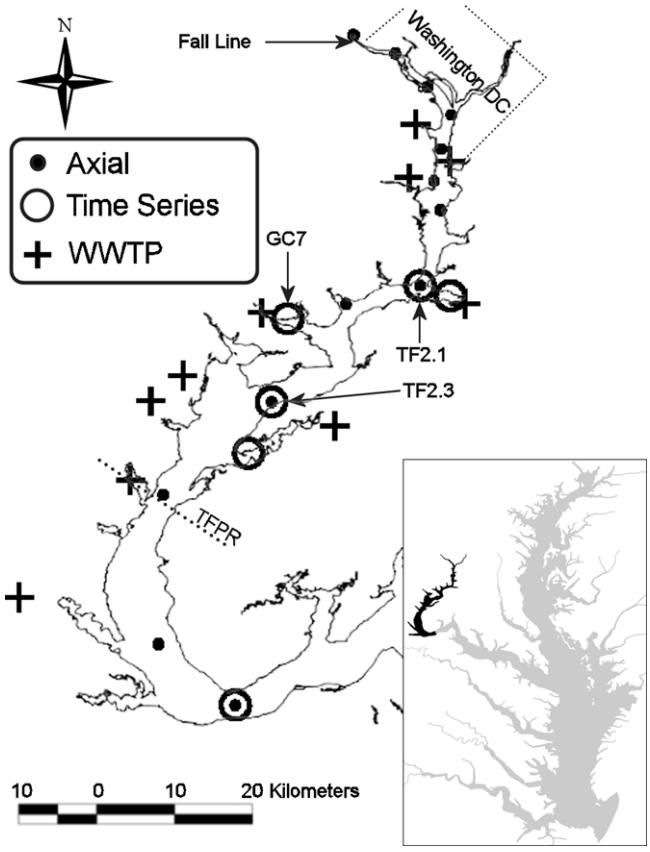

Fig. 1. The tidal fresh Potomac River showing sample stations and locations of major loadings. The inset shows the TFPR within the larger Chesapeake Bay. Sample stations used in the spatial comparison of model and observations are denoted "Axial." Sample stations used in the temporal comparison of model and observations are denoted "Time Series." "WWTP" indicates the site of a wastewater treatment plant.

et al., 1986; Lehman et al., 2008). Nutrient loading sources indirectly affect pH through their stimulation of algal blooms. They also directly influence pH through the alkalinity, inorganic carbon, and calcium carbonate they introduce to the system along with nutrients. The pH which results from the combined direct and indirect influences may attain a level sufficient to induce sediment nutrient releases, thereby stimulating and extending cyanobacteria blooms.

Analysis of the processes which influence pH and cyanobacteria blooms is facilitated through the use of a mass-balance model. The model provides a framework for constructing budgets and comparing the magnitudes of system fluxes. Model sensitivity analyses allow the step-by-step isolation of individual factors and determination of their influence. We present herein a process-based, predictive model of pH in the TFPR. The model is used to examine the hypothesis that anthropogenic influences are the major determinant of pH in the tidal fresh Potomac River. If true, this hypothesis suggests that pH can be managed through control of anthropogenic processes. The alternate hypothesis is that natural, largely uncontrollable influences are the major determinant of pH.

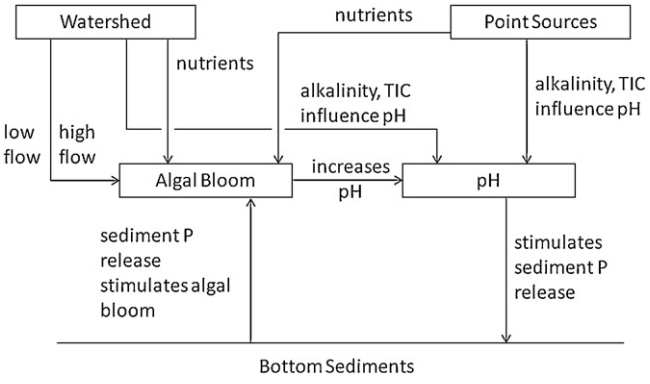

Fig. 2. Conceptual model of factors which influence pH in the tidal fresh Potomac River.

2. Materials and methods

2.1. The study site

The TFPR (Fig. 1) occupies the upper 60 km of the Potomac River estuary, which is a major sub-estuary of the Chesapeake Bay, USA. The upper and downstream boundaries of the tidal fresh portion are determined by the head of tide and by the transition from fresh to salt water (>1 ppt salinity). Although the system is tidal (mean range 0.84 m at Washington DC), it resembles a lake in several regards. The system is broad and shallow (average depth ≈4 m) with surface area (154×10^6 m^2) enhanced by numerous embayments. Hydraulic residence time approaches one year during extreme low-flow periods (Cerco and Noel, 2010). The system can be characterized as eutrophic and is subject to persistent blooms of the cyanobacteria *Microcystis aeruginosa* (Krogmann et al., 1986; Sellner, 1988). The system receives nutrient inputs from a 29,940 km^2 upland watershed and from the dense urban areas of Washington DC and its suburbs. Poor water quality, characterized by algal blooms, high turbidity, and high pH, has been a problem for decades although reductions in anthropogenic nutrient loads have produced recent improvements (Jaworski, 1990, 2007; Jones, 2008).

2.2. The Chesapeake Bay Environmental Model Package (CBEMP)

The pH model is inserted into the existing CBEMP. The CBEMP consists of three independent models: a watershed model (WSM), a hydrodynamic model (HM) and an eutrophication model (WQM). The WSM (Linker et al., 2000) provides distributed flows to the HM and nutrient and solids loads to the WQM. The HM (Johnson et al., 1993) computes three-dimensional intra-tidal transport and supplies transport parameters to the WQM on an hourly basis. The WQM (Cerco and Cole, 1993) computes algal biomass, nutrient cycling, and dissolved oxygen, as well as numerous additional constituents and processes. A predictive sediment diagenesis component (DiToro, 2001), a submerged aquatic vegetation component (Cerco and Moore, 2001), and a bivalve filtration component (Cerco and Noel, 2010) are attached to and interact with the model of the water column.

Both the HM and WQM operate on a three-dimensional grid which encompasses the entire Chesapeake Bay system. For this study, the Potomac River portion of the grid was extracted along with the associated hydrodynamics. An adjacent portion of Chesapeake Bay was included so that downstream boundary conditions could be specified at a distance sufficient to minimize influence on the upstream portions of the system. The resulting grid extended the 190 km length of the Potomac River estuary and incorporated numerous embayments and tributaries. The grid consisted of 1739 surface elements (650 m × 1300 m × 1.5 m) and 8965 total elements. A seven-year period, 1994–2000, was simulated continuously using hydrodynamic time steps of 30 s and water quality time steps of 200 s.

The extracted model was checked against the original model and against data to ensure that the extraction was performed correctly. This model version was used as a starting point for improvements to the phytoplankton component of the WQM and for pH modeling.

The formulation and validation of the WQM have been described elsewhere (Cerco et al., 2010) and will not be repeated. We concentrate here on new developments associated with pH modeling.

2.3. pH kinetics

The calculation of pH from dissolved inorganic carbon and alkalinity is a fundamental concept in aquatic chemistry (e.g. Faust and Aly, 1981) and forms the basis of the pH model. Alkalinity was defined in this freshwater system as,

$$ALK = [HCO_3^-] + 2\cdot[CO_3^{2-}] + [OH^-] - [H^+] \quad (1)$$

where $[HCO_3^-]$ = bicarbonate (mmol), $[CO_3^{2-}]$ = carbonate (mmol), $[OH^-]$ = hydronium ion (mmol), and $[H^+]$ = hydrogen ion (mmol). Alkalinity as defined in Eq. (1) is often referred to as "carbonate alkalinity" (C-Alk; e.g. Butler, 1991). The more inclusive concept of "total alkalinity" (T-Alk) includes contributions from weak acids and bases such as borates, phosphates, silicates, and ammonia (DOE, 1994). A still more inclusive concept incorporates the contribution of organic acids to T-Alk (e.g. Hunt et al., 2011). The contribution of weak acids and bases to T-Alk is commonly neglected in freshwater. Available data in the TFPR for phosphates, silicates, and ammonia confirms the validity of this assumption. No data is apparent to indicate the contribution of organic acids to T-Alk in the TFPR. The potential impact of organic acids on the study results is considered in Section 5.

To accommodate the calculation of alkalinity and of the carbonate species, four new components were added to the WQM suite of variables (Fig. 3): total inorganic carbon (TIC) including solid-phase calcium carbonate ($CaCO_3$), alkalinity (ALK) including solid-phase calcium carbonate, total calcium (TCa), and $CaCO_3$. TIC and ALK were required to compute pH. The calcium components were added to accommodate the formation and settling of $CaCO_3$ which can be an important buffer on increasing pH. All were quantified as mol m^{-3} (equivalent to mmol) except TCa as g m^{-3} (equivalent to mg L^{-1}).

The WQM operates by solving a discrete form of the three-dimensional conservation of mass equation (Cerco and Cole, 1993). The equation accounts for advection and diffusion (from the HM), external loads, and internal sources and sinks. For notational simplicity, only internal sources and sinks are listed in the relationships below.

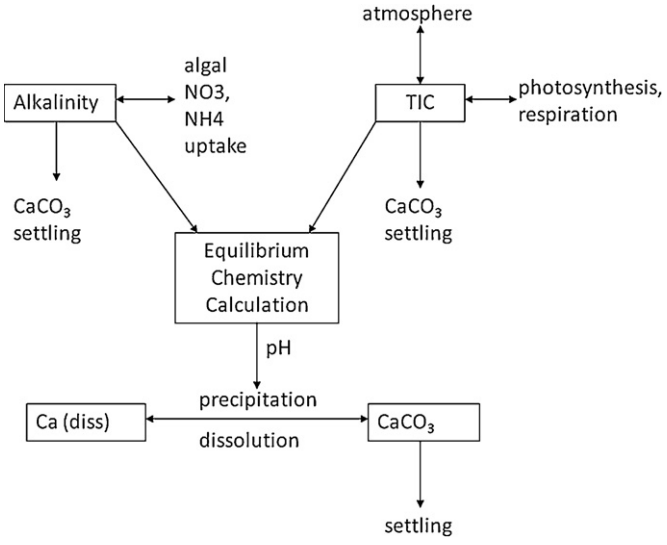

Fig. 3. The model carbonate cycle. Four new state variables, alkalinity, TIC, Ca, and $CaCO_3$, are introduced to the model suite. Photosynthesis, respiration, and algal nutrient uptake are as in the previous model version (Cerco et al., 2010). The remaining processes are new and are described herein. The equilibrium chemistry routines are adapted from Shapley and Cutler (1970).

2.3.1. Total inorganic carbon

The sources and sinks of TIC include photosynthesis/respiration by primary producers, exchange with the atmosphere, oxidation of organic matter, settling of $CaCO_3$, and respiration in the sediments. These are represented, respectively, as,

$$\Delta TIC = \frac{(R-G)\cdot P}{12} + \frac{Ka}{H}\cdot(CO_2s - CO_2) + \frac{Kd\cdot DOC}{12} - \frac{W}{H}\cdot CaCO_3 + \frac{1}{H}\cdot\frac{SOD}{2.67\cdot 12} \quad (2)$$

where R = algal respiration rate (d^{-1}), G = algal growth rate (d^{-1}), P = algal biomass (g C m^{-3}), Ka = reaeration rate (m d^{-1}), H = depth (m), CO_2s = saturation CO_2 concentration (mmol), Kd = oxidation rate of organic matter (d^{-1}), DOC = dissolved organic carbon (g C m^{-3}), W = $CaCO_3$ settling velocity (m d^{-1}), and SOD = sediment oxygen demand (g m^{-2} d^{-1}). The numerical factors convert between the native mass units employed in the rest of the WQM and the mol system employed for TIC. Submerged aquatic vegetation (SAV) and attached epiphytes influence TIC in shallow regions (depth <2 m) where water clarity and other conditions are favorable. Their influences are represented by terms similar to the algal photosynthesis/respiration term. The reaeration rate for CO_2 employs a wind-based relationship for estuaries (Hartman and Hammond, 1985).

2.3.2. Alkalinity

Processes in the water column which affect pH and ALK were summarized by Goldman et al. (1972). Several of these including methane fermentation, sulfide oxidation, and sulfate reduction can be safely neglected in the water column of the highly oxygenated, freshwater TFPR. Remaining processes include photosynthesis, respiration, nitrification, and $CaCO_3$ settling. Algal CO_2 utilization does not affect ALK as defined in Eq. (1). While direct algal uptake of bicarbonate might affect ALK, Goldman et al. (1974) argued that bicarbonate is converted to CO_2 prior to algal uptake. Rather, the primary influence of algae on ALK is through their use of NH_4^+ or NO_3^- as a nutrient (Brewer and Goldman, 1976). The OH^- ion is produced when nitrate is assimilated; the H^+ ion is produced when ammonium is assimilated. Results from Brewer and Goldman (1976) indicate ALK decreases 15 mol for every 14 mol NH_4^+ utilized and increases 17 mol for every 16 mol NO_3^- utilized. An algal affect on ALK through the use of phosphate can also be envisioned. Brewer and Goldman (1976) found this effect to be undetectable, however. Negligible effect of phosphate usage on ALK is consistent with our earlier assumption that phosphates form a negligible portion of T-Alk.

Nitrification affects ALK via the reaction,

$$2NH_4^+ + 4O_2 \rightarrow 2NO_3^- + 4H^+ + 2H_2O \quad (3)$$

The production of the H^+ ion reduces ALK (as defined in Eq. (1)) by 2 mol for each mol NH_4 nitrified. $CaCO_3$ deposition removes 2 mols ALK, as CO_3^{2-}, for every mol $CaCO_3$ removed. The ALK sources and sinks are then represented,

$$\Delta ALK = -\frac{alg\ NH_4}{14} + \frac{alg\ NO_3}{14} - 2\cdot\frac{nitrif}{14} - 2\cdot\frac{W}{H}\cdot CaCO_3 \quad (4)$$

where alg NH_4 = algal ammonium uptake (g N m^{-3} d^{-1}), alg NO_3 = algal nitrate uptake (g N m^{-3} d^{-1}), and nitrif = nitrification rate (g N m^{-3} d^{-1}). The numerical factors convert between the native mass units employed in the rest of the WQM and the mol system employed for ALK.

2.3.3. Calcium carbonate

Processes in the water column which affect $CaCO_3$ include formation and settling,

$$\Delta CaCO_3 = Kf \cdot (CaCO_3eq - CaCO_3)\gamma - \frac{W}{H} \cdot CaCO_3 \quad (5)$$

where Kf = $CaCO_3$ formation rate (d^{-1}), $CaCO_3$eq = equilibrium concentration (mmol), and γ = reaction order (≈2).

2.3.4. Total calcium

The sole internal source/sink of calcium is settling of $CaCO_3$,

$$\Delta TCa = -\frac{W}{H} \cdot CaCO_3 \cdot 40.08 \quad (6)$$

where the numerical factor converts between the mass units of total calcium and the mol units of $CaCO_3$.

2.4. Calculation of pH

The pH is calculated through solution of the classic equations for a calcium carbonate system that includes the major components [OH^-], [H^+], [H_2CO_3], [HCO_3^-], [CO_3^{2-}] as well as the calcium suite. DiToro (1976) noted that solution of time-variable mass-balance equations for each of these species presents a problem which is numerically intractable. Solution to equations for individual species is confounded by non-linearities and by the reversibility of the ionization reactions. He recommended solution of mass-balance relationships only for quantities which are unaffected by ionization reactions. These quantities include TIC, ALK, $CaCO_3$, and TCa, for which transport and transformation are computed via numerical integration using the WQM numerical schemes (Cerco and Cole, 1993). A subsequent calculation, based on local chemical equilibrium, determines the individual ionic species. Program RCHEM (Shapley and Cutler, 1970), which solves chemical composition problems based on minimizing Gibb's free energy while conserving mass and charge, is employed. The RCHEM code is incorporated into the WQM code and the equilibrium equations are solved for each cell on the computational grid at 2-h intervals. Quantities determined include the individual components of ALK, including [H^+], and $CaCO_3$.

2.5. pH–phosphorus kinetics

Following the 1983 algal bloom (Thomann et al., 1985), a mechanism was identified in which high pH stimulates sediment phosphorus release in the TFPR (Cerco, 1988; Seitzinger, 1991). Under aerobic conditions and typical pH (≈8.3), release of phosphorus from TFPR sediments is blocked by sorption of [PO_4^{2-}] ions to [Fe^{3+}] particles in surficial sediments. At higher pH, the sorption capacity is reduced and phosphorus flows freely from sediments to overlying water. This process was included in the model by incorporating pH dependence into the phosphorus partition coefficient in the sediment diagenesis model (Fitzpatrick et al., 2009),

$$\pi_{pH} = \pi \cdot \frac{4.07 \times 10^9 \cdot [H^+]}{1 + 4.07 \times 10^9 \cdot [H^+]} \quad (7)$$

where π = partition coefficient in surficial sediments, and π_{pH} = partition coefficient as influenced by pH. The relationship indicates the sorption coefficient is halved at pH = 9.6.

2.6. Data bases

The EPA Chesapeake Bay Program conducts a monitoring program throughout Chesapeake Bay and tributaries (Chesapeake Bay Program Data Hub). Stations are monitored at monthly intervals with measures conducted in situ (pH, temperature, salinity) and samples (ALK, chlorophyll) collected at various depths for later analysis. Observations at 16 stations were retrieved from an on-line data base (http://www.chesapeakebay.net/data_waterquality.aspx) and subjected to various summary procedures for comparison with the model. This data base was supplemented with observations collected in Gunston Cove (GC7, Fig. 1; Jones et al., 2008) using similar protocols and analyses. ALK was determined via titration of a sample with strong acid to pH 4.5 (Fishman and Friedman, 1985) and reported as mg L^{-1} $CaCO_3$. ALK as $CaCO_3$ was converted to mmol by noting that each mmol (100 mg) of $CaCO_3$ contains 2 mmol of ALK (Eq. (1)). Total inorganic carbon (TIC) was calculated from pH, ALK, and temperature using standard formulae (Faust and Aly, 1981). Precise calculation of TIC in saline water requires consideration of ionic activity, as well. This sophistication was unnecessary since pH is primarily of interest in the freshwater portion of the estuary and since the standard calculations were sufficiently accurate in the low-salinity waters of the estuary to set downstream boundary conditions.

2.7. Loads and boundary conditions

Monthly observations of pH, ALK, and total calcium obtained at the intake to the Dalecarlia water treatment works, located on the fluvial portion of the river immediately above the head of tide, were used to characterize concentrations of these substances entering the Potomac from the watershed. TIC was calculated as noted previously. Calcium concentrations were partitioned into dissolved and particulate (as $CaCO_3$) fractions, based on concurrent measures of pH. At the head of tide, concentrations of ALK, TIC, and calcium were converted to mass loadings through multiplication by daily volumetric flow within the model. Loads of distributed inputs, below the head of tide, were calculated on a daily basis using flows computed by the WSM and were input to the model as mass loadings.

The TFPR receives discharges from several large municipal waste treatment plants (Fig. 1). Effluent ALK, as $CaCO_3$, and pH were available at varying intervals from each plant. ALK as $CaCO_3$ was converted to mmol as described in Section 2.6. TIC was subsequently calculated from ALK and pH. Calcium was obtained by assuming all ALK was in the form of $CaCO_3$. Wastewater from each plant was characterized with median values of observed ALK and computed TIC and TCa. Characteristic concentrations were multiplied by monthly average flows at each plant to obtain mass loadings.

2.8. Sensitivity analyses

External loads to the TFPR influence pH directly and indirectly. Direct influences come through loads of TIC, ALK, and TCa. Indirect influences act through loads of nutrients and organic matter. The nutrients stimulate algal production which impacts the TIC concentration and fluxes. TIC concentration and flux are also influenced through algal and heterotrophic respiration. Additional influences and mechanisms are described in Section 2.3. Investigation of our hypothesis requires assessment of both direct and indirect influences. Multiple approaches can be taken to the sensitivity analyses. One approach is to vary inputs by an incremental amount and to examine the incremental response in model variables. A disadvantage of this approach is that the incremental changes in inputs are not necessarily relevant to the model system. The variations may be larger or smaller than variations which occur or which are feasible. We elected to base our sensitivity analyses on observed or projected endpoints to forcing functions. The influence of direct inputs from the watershed was determined by selecting the maximum and minimum monthly ALK from the simulation period. The extreme monthly ALK and corresponding TIC were employed in computing watershed loads for each month in the simulation period. Direct

Table 1
Nitrogen and phosphorus loads to the TFPR under three loading scenarios and three hydrological conditions.

	Nitrogen ($mg\,m^{-2}\,d^{-1}$)			Phosphorus ($mg\,m^{-2}\,d^{-1}$)		
	1985 point sources and land use	Existing	TMDLs	1985 point sources and land use	Existing	TMDLs
Dry hydrology						
Head of tide	46.0	43.1	39.4	1.04	0.94	0.84
Below head of tide	9.1	8.8	6.7	0.86	0.83	0.59
Point source	164.4	151.3	58.0	4.73	1.62	2.94
Total	219.4	203.3	104.1	6.63	3.39	4.37
Average hydrology						
Head of tide	149.6	148.3	105.8	24.70	24.63	15.43
Below head of tide	21.8	21.7	17.8	2.67	2.61	2.06
Point source	164.4	156.8	58.0	4.73	1.64	2.94
Total	335.7	326.8	181.7	32.10	28.88	20.43
Wet hydrology						
Head of tide	395.6	370.7	246.4	59.26	59.66	39.92
Below head of tide	22.1	22.3	18.6	2.30	2.26	1.85
Point source	164.4	160.6	58.0	4.73	1.54	2.94
Total	582.1	553.7	323.0	66.28	63.46	44.71

influences of point sources were determined by selecting the maximum and minimum monthly flows from the simulation period and applying the extreme monthly value in the computation of loads for each month in the record.

Indirect influences were evaluated from two loading extremes. The CBP has recently completed a set of Total Maximum Daily Loads (TMDLs) for the Chesapeake Bay system (US Environmental Protection Agency, 2012). The TMDLs include controls on nutrient loads from both the watershed and point sources. One limiting sensitivity run was completed using the newly developed TMDLs for the Potomac River (Table 1). In order to evaluate progress toward load reductions, the CBP compiles and computes loads from 1985, a period before major load controls were implemented. A limiting sensitivity run was constructed using point-source loads from 1985. Loads from the watershed were obtained from the WSM. The WSM computed loads based on the 1994–2000 hydrology but with 1985 land uses and control practices (Table 1). ALK and TIC loads were left at their base values while these indirect influences were examined.

2.9. Construction of budgets

Budgets for nutrients and for elements of the pH–alkalinity calculation are essential for interpreting the model results. Budgets were constructed for the TFPR, rather than the entire Potomac Estuary since pH is a concern only in the freshwater portion. The CBP divides the Chesapeake Bay system into a number of Chesapeake Bay Program Segments which are regions based on geography, characteristic salinity, and other features. The TFPR was considered to be the region designated POTTF as well as adjacent segments which encompass smaller tributaries and embayments (Fig. 1). The region extends for 60 km along the river axis, commencing 120 km from the river mouth. All budgets are reported on an areal basis, normalized by the POTTF area represented on the model grid. Budgets emphasize the summer months (June–August) since these are the months of maximum algal productivity and resulting critical water quality. We selected three summer periods for emphasis. The summer of 1994 exhibits "average" hydrology. Daily-average flow is ranked 16 in a period of 31 years, 1980–2010. The summer of 1999 represents "dry" hydrology and has the lowest daily-average flow in the 31-year interval. The summer of 1996 represents "wet" hydrology. Only one summer in the 31-year record exceeds the 1996 daily-average flow. Budgeting is computed within the model code for individual cells and assembled into a segment-wide budget in a post-processing operation.

For comparison with the model, a basic TIC budget was constructed for Station TF2.3 using observations collected in the vicinity. The budget includes algal production, water column respiration (all respiration including algae), sediment respiration, and atmospheric exchange. Details of the budget are presented in Appendix A.

3. Theory

Myriad processes influence ALK and TIC, from which pH is determined. The influence of individual processes is not readily envisioned. DiToro (2001) showed that pH is determined by the ratio of ALK to TIC (Fig. 4). The effect of individual processes on pH (Table 2) can be determined from this principle, combined with inspection of relationships in Section 2.3. Algal production increases pH through the uptake of TIC. Respiration, in the water column or sediments, reduces pH. CO_2 exchange with the atmosphere can increase or decrease pH, depending on the direction of the exchange. Two modeled processes decrease both ALK and TIC. In the case of nitrification, TIC uptake by nitrifying bacteria is negligibly small relative to the change in ALK. $CaCO_3$ deposition removes

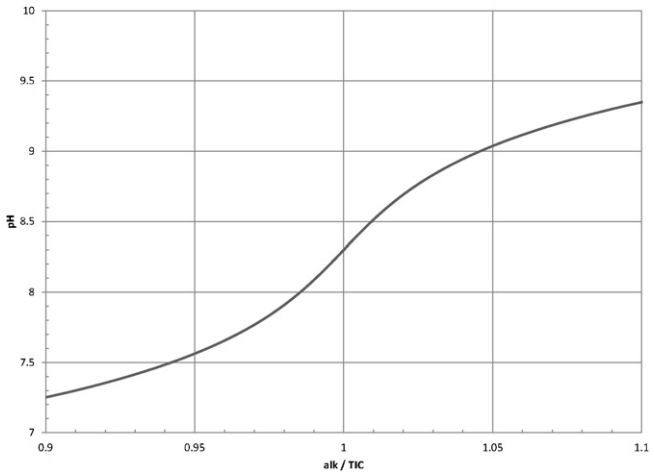

Fig. 4. The effect of the ALK/TIC ratio on pH
Redrawn from DiToro (2001).

Table 2
Effects of processes in the water column on TIC, ALK, and pH. "+" indicates an increase and "−" indicates a decrease.

Process	Effect on TIC	Effect on ALK	Effect on pH
Algal production[a]	−		+
Algal respiration	+		−
Heterotrophic respiration	+		−
Nitrification	−	−	−
Sediment oxygen consumption	+		−
Atmospheric exchange[b]	+ or −		+ or −
Calcite deposition	−	−	−

[a] SAV production and respiration have the same effects as algae.
[b] Atmospheric exchange is positive into the water column.

twice as much ALK as TIC. The net effect of both these processes is to reduce pH. Inspection of the ALK/TIC ratio can also help explain the influence of loads on receiving water. Loads in which the ratio exceeds the ratio of the receiving water will tend to increase pH; loads in which the ratio is less than the receiving water will tend to reduce pH.

4. Results

4.1. Longitudinal distribution of phytoplankton, TIC, ALK, and pH

The computed and observed longitudinal distributions of phytoplankton (as chlorophyll), TIC, ALK, and pH are shown for the summer of 1994, a year of average hydrology (Fig. 5). Both TIC and ALK decrease from the head of tide toward the downstream boundary condition. A phytoplankton bloom between km 110 and 150 produces a TIC sag in the same region. Algal uptake of TIC results in a pH increase concurrent with the algal bloom. The pre-eminent feature of the observed pH, however, is the sag between km 160 and 170. The sag occurs in the vicinity of the region's largest wastewater treatment plant (WWTP). One factor contributing to the sag is respiration of organic matter in the WWTP effluent. A second influence is the ALK/TIC ratio of the effluent. The characteristic ratio in regional WWTP effluent is less than unity and less than the ratio of water entering the system above the nearby head of tide (Table 3). As a result, according to the principle outlined in Section 3, effluent is expected to decrease pH in the vicinity of the discharge. The relative contributions of respiration and discharge ALK/TIC cannot be determined but the combined effects are obvious in the observations and in the model. The model tends to underestimate TIC in the region of the algal bloom which results in an overestimate of mean pH although the model performs well in matching the maximum observed pH in the range 8.5–9.

4.2. Time series of phytoplankton and pH

Phytoplankton chlorophyll and pH are shown at two stations which are characteristic of the TFPR (Fig. 6). One station, TF2.1, is in the mainstem of the Potomac River (H = 18 m). The second, GC7 (H = 2 m), is in a shallow tributary embayment. The shallow station is characterized by chlorophyll observations which are often double the observations in the deeper station. Peak chlorophyll concentrations are predominantly in the summer months with blooms occasionally lasting into the fall. The difference in chlorophyll concentration between the deep and shallow station is replicated in the model although the difference may be lesser in magnitude. Observed pH at the river station never attains 9.0 while this level is frequently exceeded at the shallow station and pH > 9.5 occurs in three of the seven model years. The connection between recurrent seasonal phytoplankton blooms and seasonal pH is clear in the embayment but less so in the river. In the river, seasonal behavior in pH is more apparent in extreme rather than mean values. The model reproduces a direct connection between phytoplankton blooms and pH although the connection is exaggerated at the riverine station.

4.3. ALK, TIC, and pH summaries

The overall characteristics of the system and of its model are difficult to ascertain from comparisons at individual stations. Summary graphics are required. The summaries employed here are cumulative distribution plots. These were created by pairing in space and time the observations and computations from time series stations (Fig. 1). The pairs were combined into two populations, representing the river and embayments, and sorted from smallest to largest. The sorted arrays were divided into quantiles and plotted as cumulative distributions (Fig. 7). Any point in the distribution indicates the percentage of observations or computations less than the indicated concentration. Median values occur at 50% of the cumulative distribution.

Agreement between computed and observed ALK at the river stations is superior to the embayment stations. The superior performance in the river is attributed to the availability of ALK observations near the major inflow and to the predominance of the inflow on the ALK budget (Table 3). Absence of local observations

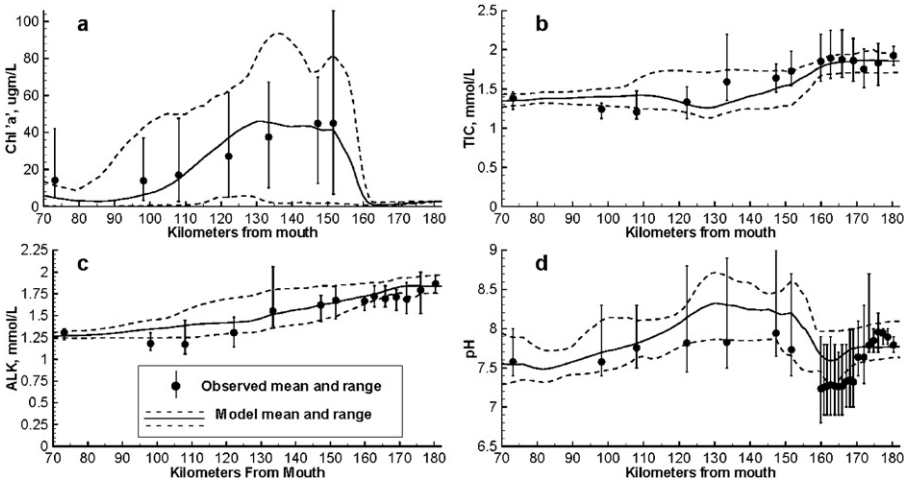

Fig. 5. Computed and observed: (a) surface chlorophyll; (b) TIC; (c) ALK; and (d) pH along the channel of the Potomac River, June–August 1994. The tidal fresh portion commences 120 km above the river mouth.

Table 3
Model TIC and ALK budgets under three hydrological conditions. TIC fluxes derived from observations are obtained from Appendix A.

	TIC (mmol m^{-2} d^{-1})			ALK (mmol m^{-2} d^{-1})			ALK/TIC, average hydrology	Observed TIC flux
	Dry hydrology	Average hydrology	Wet hydrology	Dry hydrology	Average hydrology	Wet hydrology		
Head of tide	19.2	171.0	438.3	23.1	176.3	421.2	1.03	
Below head of tide	4.9	32.9	28.6	6.0	31.7	27.4	0.96	
Point source	23.1	22.3	22.3	15.1	16.1	16.1	0.72	
Algal production	−310.4	−235.5	−149.6	−18.6	−11.4	−6.2		−270
Algal respiration	177.1	123.0	88.4					
Water column respiration	83.0	55.7	36.0					104
Nitrification	−0.4	−0.4	−0.3	−9.2	−7.7	−7.7		
Aquatic vegetation	−5.8	−4.5	−2.6	−0.3	−0.2	−0.1		
Sediment–water exchange[a]	39.7	30.7	25.2	−15.9	−16.9	−7.0		47
Atmospheric–water exchange	−7.7	−15.8	−35.8					−13
Sum of loads[b]	47.2	226.3	489.2	44.2	224.1	464.7		
Sum of water column	−24.7	−46.8	−38.8	−43.9	−36.3	−21.0		
Export downstream	−8.5	−171.4	−439.8	−17.5	−189.1	−446.4		

[a] Sediment–water exchange includes respiration and $CaCO_3$ deposition.
[b] Loads, water column kinetics, and export do not sum to zero due to change in concentration and small round-off error.

forced the use in the embayments of the same observations that were used to characterize watershed loads to the river. For these systems, watershed inputs may differ due to local characteristics.

Model estimates of TIC fall short, by ≈0.1 mmol, systemwide. In the river, the shortfall of TIC results in an overestimate of pH, ≈0.2 pH units at the median of the observed and computed distributions. For the embayments, the simultaneous underestimation of ALK and TIC in the model produces accurate estimates of pH which coincide with the observed distribution throughout most of the range.

4.4. Hydrological effects on budgets of TIC and ALK

The system TIC budget transitions from dominance by loads to dominance by phytoplankton activity as the hydrology transitions from wet to dry conditions (Table 3). Algal activity is greatest when watershed runoff is least, indicating the effect of hydraulic residence time on algal production. At low flows, the residence time is lengthy, providing ample opportunity for algal blooms to persist. The blooms persist despite the fact that runoff and nutrient loads co-vary. The intervals of greatest residence time are the intervals of least watershed nutrient loading (Table 1). Algal production and respiration are the greatest in-stream fluxes of TIC under any circumstances and TIC uptake via algal production exceeds production via algal respiration by nearly a factor of two. The model TIC budget demonstrates good agreement, in flux magnitude and direction, with the independent budget derived in Appendix A. Both budgets indicate algal production is the largest flux in magnitude and exceeds respiration by a factor of two or more. Both budgets agree that the water column looses TIC to the atmosphere. As noted in Appendix A, the TIC deficit in the budget derived from observations implies the existence of a TIC source not considered. The model budget indicates the source is TIC flowing in from the watershed above the head of tide.

External loads provide the only source of ALK to the system and the watershed predominates over point sources even under dry conditions. Under average to wet hydrology, ALK loads greatly exceed water column sinks and the majority of the ALK load passes downstream. Sinks in the water column compare in magnitude with loads only under extremely dry conditions. The model still computes ALK export downstream, with the apparent ALK deficit supplied by a decrease in concentration over the season.

4.5. Sensitivity analyses

The TFPR is an extensive system with complex geometry and flow patterns. Local conditions within the system are determined not only by geometry and flows but by local loads of nutrients, organic matter, ALK and TIC from the watershed and point sources. We construct summaries here through the use of cumulative

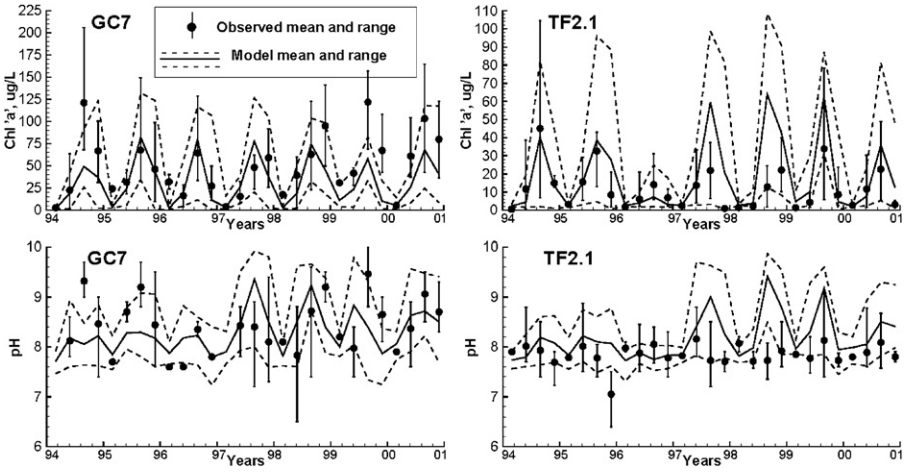

Fig. 6. Computed and observed chlorophyll and pH at two contrasting stations: TF2.1 in the channel of the TFPR and GC7 in the Gunston Cove embayment.

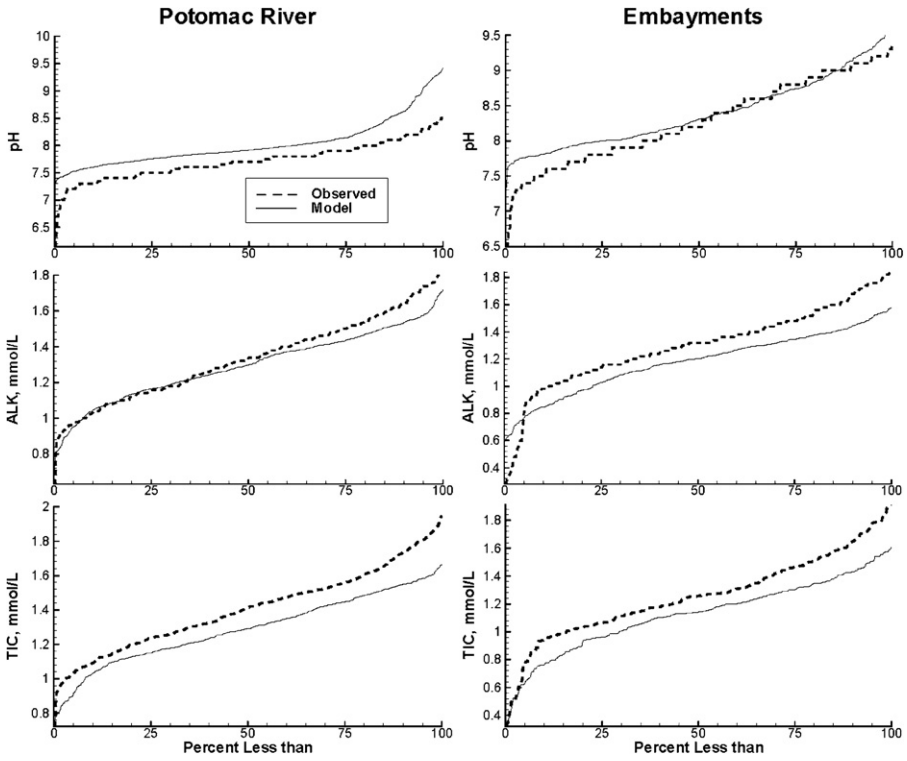

Fig. 7. Cumulative distributions of computed and observed ALK, TIC, and pH for two groupings: stations in the channel of the TFPR and stations in adjoining embayments.

distribution charts. In this case, the population consists of daily-average computed values in each TFPR grid cell for each day of the summer months June–August. The population is sorted from smallest to largest, divided into quantiles, and plotted as a cumulative distribution. The base case in each analysis is the population of ALK, TIC, or pH in the summer of the average hydrological year, 1994.

4.5.1. Sensitivity to environmental influences

Hydrology has the greatest computed effect on pH of all the factors examined (Fig. 8a). Median computed pH in the dry year, 1999, is 1.2 units higher than in the wet year 1996. As noted in Section 4.4, the residence time during the dry year is lengthy allowing ample time for algal production, net uptake of TIC, and enhanced pH. ALK and TIC in runoff are additional factors which contribute to environmental variation in pH. During the summer of a 1994, watershed ALK and TIC were close to their maximum values so that a sensitivity run completed using maximum monthly values shows little difference in resulting pH. The median summer pH values are identical (Fig. 8b). The minimum observed monthly ALK and TIC values were less than occurred in 1994. Substitution of the minimum values into the model loading file results in an increase of ≈0.2 units in median pH.

4.5.2. Sensitivity to anthropogenic influences

Substitution of limiting values of nutrient loads into the model has no effect on the loadings of ALK and TIC. Concentration changes

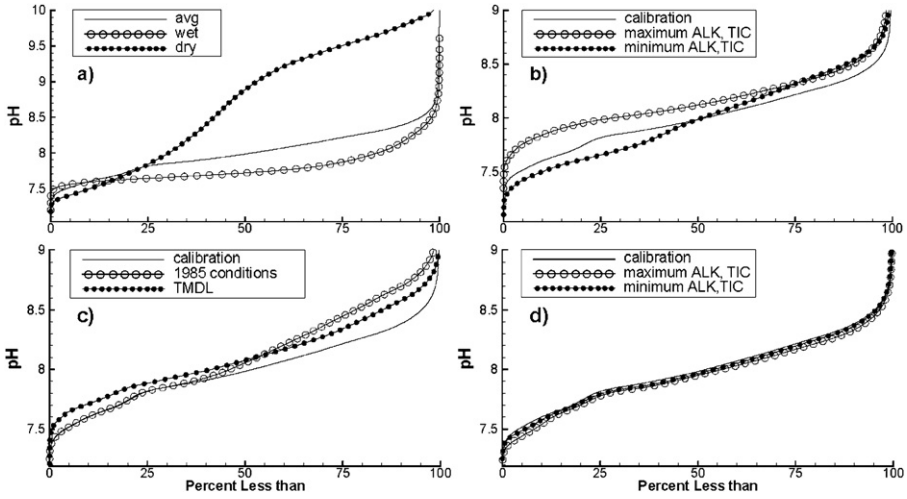

Fig. 8. Cumulative distributions of computed pH in the TFPR for four sensitivity analyses: (a) pH computed in dry, average, and wet hydrological conditions; (b) sensitivity, under average hydrological conditions, to extremes in watershed ALK and TIC; (c) sensitivity, under average hydrological conditions, to feasible extremes in nutrient loading; (d) sensitivity, under average hydrological conditions, to ALK and TIC loads from regional wastewater treatment plants.

in these two substances, and subsequent effects on pH, are due to the influence of nutrients on algal production as well as other changes in water column kinetics induced by the load alterations. According to our hypothesis, an increase in nutrient loading should increase pH due to stimulation of algal production. During an interval of average hydrology, the increase in median pH induced by using the higher 1985 nutrient loads is ≈0.1 pH units (Fig. 8c). The excess of pH increases in the upper range of the distribution. This phenomenon indicates the existence of "hot spots" where the lower existing nutrient loads produce benefits through limitation of algal production. Computed pH with the TMDL loads is higher than with existing loads throughout the distribution. Median pH with TMDL loads is equivalent to median pH with 1985 loads. The behavior counters the expectation that pH would decrease due to diminished algal production. Diminished algal production does, in fact, result from the lower nutrient loads. Two factors confound corresponding reduction in pH, however. The first is a decrease in TIC production from sediment respiration, indicating that less organic matter is deposited on the bottom. The second factor is an increase in production by aquatic vegetation, stimulated by reduction in light attenuation from organic and inorganic solids in the water column. Implementation of TMDL loads produces a net decrease in TIC and a resulting 0.1 unit increase in pH.

ALK and TIC resulting from the use of minimum WWTP flows are nearly identical to the values produced by actual 1994 WWTP flows. ALK and TIC are both increased when maximum WWTP flows are employed, consistent with the higher loading. The increases are small, however, less than 0.1 mmol each and result in virtually no alteration in computed pH. Overall, the change in alteration in median pH between minimum and maximum WWTP flows is less than 0.1 pH units.

5. Discussion

Exact replication of pH observations with a mathematical model is a challenge. The pH depends on phytoplankton biomass and production which are difficult to compute precisely in time and space. The pH computation also depends on ALK and TIC loading and boundary conditions for which detailed information is not always available. Nevertheless, the model provides a framework for examination of the processes which determine pH and for determination of magnitude and direction of pH response to alterations in forcing functions.

Our model combines a spatially and temporally resolved eutrophication model with a comparably resolved model of the carbonate cycle. Our model is one of the more complex, when compared to similarly focused, contemporary representations of alternate systems. At one extreme of model complexity, estuarine pH was calculated based on conservative mixing of river and seawater end members (Mosley et al., 2010). This approach is unsuited for the TFPR since it ignores biological activity and distributed loads of ALK and TIC. Multi-dimensional combined models comparable to our own have been applied to the North and Baltic Seas. The North Sea model constrains calculated ALK, based on observed values, with the aim of accurately computing air–sea CO_2 flux (Prowe et al., 2009). The Baltic Sea model (Omstedt et al., 2009) most closely resembles our own in formulation and results although it is, perhaps, more complex since it considers constituents (e.g. boron) and processes (e.g. water column denitrification) which can be neglected in the TFPR. Our representation is distinguished from the North and Baltic Seas by the importance of nutrient and ALK loads from WWTPs and from the heterogeneous watershed which adjoins the river from the mouth to the head of tide.

Our model represents the present state of the art for computation of the carbonate cycle in the TFPR. The primary constraints on accuracy are attributed to data limitations and inherent variability in the biological processes which affect the carbonate cycle. A comprehensive data base exists for model application in the TFPR. Monitoring and observations include loads from the major upland watershed, loads from wastewater discharges, in situ concentrations of chlorophyll, nutrients, ALK and pH, and measures of primary production, respiration, and sediment oxygen consumption. Still, few or no observations are available for specific elements of the carbonate cycle. Calcium observations are available to characterize the loads at head of tide but are lacking in the point-source loads and in the water column. Under conditions of average hydrology, the TCa load at the head of tide is 0.60 $g\,m^{-2}\,d^{-1}$ compared to 0.32 $g\,m^{-2}\,d^{-1}$ from WWTPs. Since the TCa loads are dominated by loads at the head of tide, which are monitored, the approximation employed to obtain point-source TCa (Section 2.7) is of little consequence. During dry hydrology, however, the point-source TCa load represents a greater proportion of the total loading and our calculation of pH buffering by $CaCO_3$ formation may be affected. Absent measures of TCa or $CaCO_3$ in the water column, the model parameters which determine calcite formation and settling can be only approximately evaluated. We attempted to improve the pH computation by varying parameters related to $CaCO_3$ formation and found little sensitivity of calculated pH to these parameters. Consequently, the ability to assign parameter values based on observed TCa and/or $CaCO_3$ would not necessarily improve model accuracy but would refine the estimates of terms involving $CaCO_3$ in the TIC and ALK budgets and promote confidence in the model formulation and parameterization.

No data is apparent to indicate the contribution of organic acids to T-Alk in the TFPR. A study of rivers in the Northeastern US and Canada found the contribution of non-carbonate alkalinity to the total declined as pH increased from acid to neutral conditions (Hunt et al., 2011). Non-carbonate alkalinity was 10–20% of the total alkalinity at pH ≈ 7.5, the highest pH examined. Neutral pH is the minimum value of concern in the TFPR with basic conditions prevailing. If we assume the results from the northeastern rivers can be extended to the TFPR, then the contributions of organic acids to T-Alk would be on the order of 10%. The primary effect of the presence of organic acids identified by Hunt et al. (2011) was an over-estimation of the CO_2 partial pressure calculated from T-Alk and pH. The CO_2 concentration is determined by calculation in this study and over-estimation would result in exaggeration of the amount of TIC lost to the atmosphere. This term is small, however relative to algal production, respiration, and fall-line loading (Table 3). Consequently the major terms of the TIC budget and the relative magnitude of the terms are likely unaffected by the presence of organic acids in the TFPR. Hunt et al. (2011) noted that only half of the organic acids were detected by titration to the 2–4 pH range. Again extending from the northeastern rivers and employing our estimate of 10% contribution of organic acids to T-Alk, an additional 10% of T-Alk may be undetected in the titration of TFPR samples to pH 4.5. This additional ALK has little impact on the ALK budget (Table 3); loading and export remain the dominant terms. A potentially more significant effect would be to alter and increase the ALK/TIC ratio of the loads thereby increasing the tendency of the system to elevated pH (Fig. 4).

Our initial hypothesis was that anthropogenic influences are the primary determinant of pH in the tidal fresh Potomac River. The major anthropogenic influence is nutrient loading which stimulates algal production, results in net TIC uptake, and increases pH. Investigation with the model favors the alternate hypothesis. Variations in pH due to environmental influences, largely hydrology, are greater than variations attributable to anthropogenic influences. Hydrology acts on pH via residence time. The pH is higher during low flow periods, when algae have ample time to form blooms, than

during high flow periods even though nutrient loading is greater during high flows.

Nutrient loads from WWTPs are expected to increase or diminish pH through stimulation or limitation of algal production. Model sensitivity runs based on 1985–1999 reductions in total nutrient loads indicate the corresponding reduction in median pH is ≈0.1 during summer of an average hydrologic year (Fig. 8c). Sensitivity runs indicate further nutrient reductions may cause median pH to climb back ≈0.1 units due to diminished sediment respiration and increased photosynthesis from aquatic vegetation (Fig. 8c). This increase is speculative since it is derived from complex model interactions which are difficult to validate. Nevertheless, the change in median pH due to feasible changes in total nutrient loads is characterized by ±0.1 pH units. Since the WWTP nutrient loads comprise only a portion of the total, the variation in median pH attributable to WWTP loads is minimal. An unexpected influence of WWTPs on pH is apparent in the data (Fig. 5), independent of the model; a pH sag occurs in the vicinity of the region's largest WWTP, between km 160 and 170. Subsequent model analysis indicates the sag is induced by TIC production during respiration of effluent organic matter and by the low effluent ratio of ALK to TIC. From a regional perspective, however, ALK and TIC loads from point sources are small and exert little influence on comprehensive summaries of pH (Fig. 8d).

6. Conclusions

Hydrology is the major determinant of pH in the TFPR. Median computed pH during dry and wet extremes varies by 1.2 units above and below the median in a season of average hydrology. Hydrology acts on pH via residence time. During intervals of low flow, residence time is long, algal production is enhanced, and pH rises due to algal TIC uptake. During intervals of high flow, algae are washed out before blooms can occur and algal TIC uptake is minimal. Potential variations in ALK and TIC from the watershed are the secondary influences on computed pH. Computed median pH varies by ≈0.2 units in a summer of average hydrology when extreme values of watershed ALK and TIC are employed in the model. Lesser influences on computed pH in an average year are variations in nutrient loading and variations in ALK and TIC loading from regional WWTPs.

Acknowledgements

The authors thank Dominic DiToro for pointing out the influence of the ALK/TIC ratio on pH. The pH–alkalinity algorithms employed here were initially developed by Dominic DiToro and James Fitzpatrick. The phytoplankton component of the model was parameterized by Victor Bierman and Amanda Flynn. R. Christian Jones contributed observations collected in Gunston Cove and adjacent waters. This study was sponsored by the US Environmental Protection Agency Chesapeake Bay Program.

Appendix A. Observed total inorganic carbon fluxes

Elements of the TIC budget which can be derived from observations include: (1) algal production; (2) water column respiration; (3) sediment respiration; and (4) atmospheric exchange. These were calculated using parameters typical for the TFPR during summer of 1994, a year of average hydrology.

A.1. Algal production

The fundamental measure of algal production is light-saturated algal carbon fixation, Cfix, observed at Station TF2.3 (Chesapeake Bay Program Data Hub). These short-term measures (Strickland and Parsons, 1972) are interpreted as the maximum algal production under ambient nutrient conditions and no light limitation. Conversion of the in vitro measures to daily values in the water column requires integration over daylength and depth, accounting for light limitation due to diurnal variation in solar irradiance and attenuation in the water column (Table A1). The relationships for instantaneous irradiance and for light limitation were derived from the model code. Irradiance was assumed to decline exponentially with depth due to ambient light attenuation. Relationships, parameter values, and their sources used to calculate a typical summer value of daily algal carbon fixation are reported in Table A1.

A.2. Respiration

The fundamental measures of water column respiration were BOD observations conducted in the vicinity of Station TF2.3 (Boynton and Bailey, 2008). These were converted from oxygen consumption to CO_2 production, using a respiration quotient 2.67 g O_2 g^{-1} C, and integrated over depth, assuming no vertical variation in respiration (Table A2). Measures of sediment oxygen demand in the vicinity of TF2.3 (Boynton and Bailey, 2008) were converted to CO_2 production using the same respiration quotient as employed in the water column.

Table A1
Derivation of the effect of phytoplankton production on TIC based on observations collected in the vicinity of Station TF2.3 during June–August.

Parameter	Definition	Value	Source
H	Depth	5.2 m	Model grid
Cfix	Light-saturated algal carbon fixation	10 g C m^{-3} d^{-1}	Chesapeake Bay Program Data Hub
Kd	Light attenuation	2 m^{-1}	Chesapeake Bay Program Data Hub
It	Total daily irradiance	44 E m^{-2}	Fisher et al. (2003)
FD	Daylight fraction	0.6	Calculated from latitude and day of year
Io(t)	Instantaneous surface irradiance		$\mathrm{Io}(t) = \frac{\pi}{2 \cdot \mathrm{FD}} \cdot \mathrm{It} \cdot \sin\left(\frac{\pi \cdot t}{\mathrm{FD}}\right)$ t = time since sunrise, in fractional days
$I(z,t)$	Irradiance at depth z, time t		$I(z,t) = \mathrm{Io}(t) \cdot e^{-\mathrm{Kd} \cdot z}$
Ik		50 E m^{-2} d^{-1}	Model value
$f(I)$	Instantaneous light limit to algal production		$f(I) = \frac{I(x,t)}{\sqrt{I(z,t)^2 + \mathrm{Ik}^2}}$
Alg P	Daily algal production	3.26 g C m^{-2} d^{-1}, 0.27 mol C m^{-2} d^{-1}	$\mathrm{Alg\,P} = \int_{\mathrm{tsr}}^{\mathrm{tss}} \int_0^H \mathrm{Cfix} \cdot f(I)\, dz\, dt$ tsr = time of sunrise, in fractional days tss = time of sunset, in fractional days

Table A2
Derivation of the effect of water column and sediment respiration on TIC based on observations collected in the vicinity of Station TF2.3 during June–August.

Parameter	Definition	Value	Source
Rvol	Water column volumetric respiration	0.64 g DO m^{-3} d^{-1}	Measured at station PT19, PT21 (Boynton and Bailey, 2008)
R	Water column areal respiration	1.25 g C m^{-2} d^{-1}, 0.104 mol C m^{-2} d^{-1}	$R = \text{Rvol} \cdot H \cdot \frac{\text{gC}}{2.67\,\text{gDO}}$
SOD	Sediment oxygen demand	1.5 g DO m^{-2} d^{-1}	Measured at HGNK (Boynton and Bailey, 2008)
Rsed	Sediment respiration	0.56 g C m^{-2} d^{-1}, 0.047 mol C m^{-2} d^{-1}	$\text{Rsed} = \text{SOD} \cdot \frac{\text{gC}}{2.67\,\text{gDO}}$

Table A3
Derivation of the atmosphere–water TIC exchange based on observations collected in the vicinity of Station TF2.3 during June to August.

Parameter	Definition	Value	Source
W	Wind speed	3.2 m s^{-1}	Typical value from meteorological observations
Kr	Exchange coefficient	2 m d^{-1}	Calculated from Hartman and Hammond (1985) at 28 °C. Assume wind over water is 1.5 × wind at land station
$CO_2(s)$	Saturated CO_2 concentration	0.01 mol m^{-3}	Calculated value at 28 °C
TIC	Total inorganic carbon	1.5 mol m^{-3}	Typical value at station TF2.3, calculated from observed pH, alkalinity
$^{\alpha}H_2CO_3$	Fraction of TIC in the form of CO_2	0.011	Tabulated at pH 8.3 (Faust and Aly, 1981)
CO_2	Water column CO_2 concentration	0.0165 mol m^{-3}	$CO_2 = {}^{\alpha}H_2CO_3 \cdot CO_2(s)$
CO_2 flux	Atmosphere–water CO_2 exchange, positive into water column	−0.013 mol m^{-2} d^{-1}	$CO_2\ \text{flux} = \text{Kr} \cdot (CO_2(s) - CO_2)$

A.3. Atmospheric exchange

An in situ value of TIC was derived from observed pH and alkalinity at Station TF2.3 (Table A3) and the CO_2 fraction was determined from standard tabulations (Faust and Aly, 1981). The exchange rate with the atmosphere was calculated from the relationship of Hartman and Hammond (1985) using parameter values reported in Table A3.

The largest element in the TIC budget is algal production which removes from the water column twice as much TIC as is produced through combined respiration in the water and sediments. The water surface is supersaturated with CO_2, however, so that the gas vents to the atmosphere. The budget indicates a CO_2 deficit since combined algal uptake and losses to the atmosphere exceed production via respiration.

References

Bailey, E., Owens, M., Boynton, W., Cornwell, J., Kiss, E., Smail, P., Soulen, H., Buck, E., Ceballos, M., 2006. Sediment phosphorus flux: pH interaction in the tidal freshwater Potomac River Estuary. University of Maryland Center for Environmental Science TS-505-06-CBL, Solomons, MD.

Borges, A., Gypens, N., 2010. Carbonate chemistry in the coastal zone responds more strongly to eutrophication than to ocean acidification. Limnology and Oceanography 55 (1), 346–353.

Butler, J., 1991. Carbon Dioxide Equilibria and Their Applications. Lewis Publishers, Chelsea, MI.

Brasse, S., Nellen, M., Seifert, R., Michaelis, W., 2002. The carbon dioxide system in the Elbe estuary. Biogeochemistry 59, 25–40.

Brewer, P., Goldman, J., 1976. Alkalinity changes generated by phytoplankton growth. Limnology and Oceanography 21 (1), 108–117.

Caldeira, K., Wickett, M., 2003. Anthropogenic carbon and ocean pH. Nature 425, 365.

Cerco, C., 1988. Sediment nutrient fluxes in a tidal freshwater embayment. Water Resources Bulletin 24 (2), 255–260.

Cerco, C., Cole, T., 1993. Three-dimensional eutrophication model of Chesapeake Bay. Journal of Environmental Engineering 119 (6), 1006–1025.

Cerco, C., Moore, K., 2001. System-wide submerged aquatic vegetation model for Chesapeake Bay. Estuaries 24 (4), 522–534.

Cerco, C., Noel, M., 2010. Monitoring, modeling, and management impacts of bivalve filter feeders in the oligohaline and tidal fresh regions of the Chesapeake Bay system. Ecological Modelling 221, 1054–1064.

DiToro, D., 1976. Combining chemical equilibrium and phytoplankton models – a general methodology. In: Canale, R. (Ed.), Modeling Biogeochemical Processes in Aquatic Systems. Ann Arbor Science, Ann Arbor, MI, pp. 233–255.

DiToro, D., 2001. Sediment Flux Modeling. Wiley-Interscience, New York.

DOE, 1994. In: Dickson, A.G., Goyet, C. (Eds.), Handbook of Methods for the Analysis of the Various Parameters of the Carbon Dioxide System in Sea Water. Version 2. ORNL/CDIAC-74. Oak Ridge National Laboratory, Oak Ridge TN, USA.

Faust, S., Aly, O., 1981. Chemistry of Natural Waters. Ann Arbor Science, Ann Arbor, MI.

Fisher, T., Gustafson, A., Radcliffe, G., Sundberg, K., Stevenson, J., 2003. A long-term record of photosynthetically active radiation (PAR) and total solar energy at 38.6° N, 78.2° W. Estuaries 26, 1450–1460.

Fishman, M., Friedman, L., 1985. Methods for Determination of Inorganic Substances in Water and Fluvial Sediments. US Geological Survey Open File Report 85-495, Washington, DC.

Gao, Y., Cornwell, J., Stoecker, D., Owens, M., 2012. Effects of the cyanobacterial-driven pH increases on sediment nutrient fluxes and coupled nitrification–denitrification in a shallow fresh water estuary. Biogeosciences 9, 2697–2710.

Goldman, J., Porcella, D., Middlebrooks, E., Toerjen, D., 1972. The effect of carbon on algal growth – its relationship to eutrophication. Water Research 6, 637–679.

Goldman, J., Oswald, W., Jenkins, D., 1974. The kinetics of inorganic carbon limited algal growth. Journal of the Water Pollution Control Federation 46 (3), 554–574.

Hartman, B., Hammond, D., 1985. Gas exchange in San Francisco Bay. Hydrobiologia 129, 59–68.

Hunt, C., Salisbury, J., Vandemark, D., McGillis, W., 2011. Contrasting carbon dioxide inputs and exchange in three adjacent New England estuaries. Estuaries and Coasts 34, 68–77.

Jaworski, N., 1990. Retrospective study of the water quality issues of the upper Potomac Estuary. Reviews in Aquatic Sciences 3 (2), 11–40.

Johnson, B., Kim, K., Heath, R., Hsieh, B., Butler, L., 1993. Validation of the three-dimensional hydrodynamic model of Chesapeake Bay. Journal of Hydraulic Engineering 119 (1), 2–20.

Jones, R.C., 2008. Long-term response of water quality to changes in nutrient loading at a mainstem site in the tidal freshwater Potomac River. Verhandlungen des Internationalen Verein Limnologie 30 (4), 633–637.

Jones, R.C., Kelso, D., Schaeffer, E., 2008. Spatial and seasonal patterns in water quality in an embayment-mainstem reach of the tidal freshwater Potomac River, USA: a multiyear study. Environmental Monitoring and Assessment 147, 351–375.

Krogmann, D., Butalla, R., Sprinkle, J., 1986. Blooms of cyanobacteria on the Potomac River. Plant Physiology 80, 667–671.

Lehman, P., Boyer, G., Satchwell, M., Waller, S., 2008. The influence of environmental conditions on the seasonal variation of *Microcystis* cell density and microcystins concentration in the San Francisco Estuary. Hydrobiologia 600, 187–204.

Linker, L., Shenk, G., Dennis, R., Sweeney, J., 2000. Cross-media models of the Chesapeake Bay watershed and airshed. Water Quality and Ecosystems Modeling 1 (1–4), 91–122.

Lung, W., 1987. Lake acidification model: practical tool. Journal of Environmental Engineering 113 (4), 900–915.

Mosley, L., Peake, B., Hunter, K., 2010. Modelling of pH and inorganic carbon speciation in estuaries using the composition of the river and seawater end members. Environmental Modelling and Software 25, 1658–1663.

Nikolaidis, N., Schnoor, J., Georgakakos, K., 1989. Modeling of long-term lake alkalinity responses to acid deposition. Journal of the Water Pollution Control Federation 61, 188–199.

Omstedt, A., Gustafsson, E., Wesslander, K., 2009. Modelling the uptake and release of carbon dioxide in the Baltic Sea surface water. Continental Shelf Research 29, 870–885.

Passell, H., Dahm, C., Bedrick, E., 2007. Ammonia modeling for assessing potential toxicity to fish species in the Rio Grande, 1989–2002. Ecological Applications 17 (7), 2087–2099.

Prowe, A., Thomas, H., Pätsch, J., Kühn, W., Bozec, Y., Schiettecatte, L.-S., Borges, A., de Baar, H., 2009. Mechanisms controlling the air–sea CO_2 flux in the North Sea. Continental Shelf Research 29, 1801–1808.
Seitzinger, S., 1991. The effect of pH on the release of phosphorus from Potomac estuary sediments: implications for blue-green algal blooms. Estuarine, Coastal and Shelf Science 33, 409–418.
Sellner, K., 1988. Effects of increasing salinity on a cyanobacteria bloom in the Potomac River estuary. Journal of Plankton Research 10 (1), 49–61.
Shapley, M., Cutler, L., 1970. Rand's Chemical Composition Program: A Manual. Rand Corp Memo 495-PR, Santa Monica, CA.
Soetaert, K., Hofmann, A., Middelburg, J., Meysman, F., Greenwood, J., 2007. The effect of biogeochemical processes on pH. Marine Chemistry 105, 30–51.
Strickland, J., Parsons, T., 1972. A Practical Handbook of Seawater Analysis, 2nd edition. Bull. Fish. Res. Board Can. 167, 1–310.
Thomann, R., Jaworski, N., Nixon, S., Paerl, H., Taft, J., 1985. The 1983 Algal Bloom in the Potomac Estuary. Potomac Strategy State/EPA Management Committee, Washington, DC.
Waldbusser, G., Voigt, E., Bergschneider, H., Green, M., Newell, R., 2011a. Biocalcification in the eastern oyster (*Crassostrea virginica*) in relation to long-term trends in Chesapeake Bay pH. Estuaries and Coasts 34, 221–231.
Waldbusser, G., Steenson, R., Green, M., 2011b. Oyster shell dissolution rates in estuarine waters: effects of pH and shell legacy. Journal of Shellfish Research 30 (3), 659–669.
Weber, W., Stumm, W., 1963. Mechanism of hydrogen ion buffering in natural waters. Journal of the American Water Works Association 55, 1553–1578.

Web references

Boynton, W., Bailey, E., 2008. Sediment Oxygen and Nutrient Exchange Measurements from Chesapeake Bay, Tributary Rivers and Maryland Coastal Bays: Development of a Comprehensive Database & Analysis of Factors Controlling Patterns and Magnitude of Sediment–Water Exchanges. http://www.gonzo.cbl.umces.edu/data.htm (last accessed December 2012).
Cerco, C., Kim, S.-C., Noel, M., 2010. The 2010 Chesapeake Bay eutrophication model. A report to the US Environmental Protection Agency Chesapeake Bay Program and the US Army Engineer Baltimore District. http://www.chesapeakebay.net/content/publications/cbp_55318.pdf (last accessed December 2012).
Fitzpatrick, J., DiToro, D., Wu, B., 2009. Bloom of *Microcystis aeruginosa* in the upper Potomac River estuary: interactions between primary productivity, pH and sediment phosphorus release. In: Proceedings of 13th World Lake Conference Wuhan China, http://www.ilec.or.jp/eg/wlc/wlc13/wlc13papers2.html (last accessed December 2012).
Jaworski, N., 2007. Potomac River Treatise. http://www.potomacriver.org/2012/wildlifedocs/NAJ_00_FrontCover_TOC.pdf (last accessed December 2012).
US Environmental Protection Agency, 2012. Chesapeake Bay TMDL. http://www.epa.gov/reg3wapd/tmdl/ChesapeakeBay/tmdlexec.html (last accessed December 2012).
USEPA Chesapeake Bay Program Data Hub. http://www.chesapeakebay.net/data (last accessed December 2012).